Stereoselective copolymerization of styrene with terpenes catalyzed by an ansa-lanthanidocene catalyst: Access to new syndiotactic polystyrene-based materials

E. Laur, A. Welle, A. Vantomme, J.-M. Brusson, J.-F. Carpentier, E. Kirillov

catalysts

MDPI

Article

Stereoselective Copolymerization of Styrene with Terpenes Catalyzed by an *Ansa*-Lanthanidocene Catalyst: Access to New Syndiotactic Polystyrene-Based Materials

Eva Laur [1], Alexandre Welle [2], Aurélien Vantomme [2], Jean-Michel Brusson [3], Jean-François Carpentier [1,*] and Evgueni Kirillov [1,*]

1 Institut des Sciences Chimiques de Rennes, CNRS, Université de Rennes, UMR 6226, F-35042 Rennes, France; eva.laur@univ-rennes1.fr

2 Total Raffinage Chimie Research, Zone Industrielle C, B-7181 Feluy, Belgium; alexandre.welle@univ-rennes1.fr (A.W.); Aurelien.vantomme@univ-rennes1.fr (A.V.)

3 Total S.A., Direction scientifique, 24 Cours Michelet, F-92069 Paris La Défense CEDEX, France; jean-Michel.Brusson@univ-rennes1.fr

* Correspondence: jean-francois.carpentier@univ-rennes1.fr (J.-F.C.); evgueni.kirillov@univ-rennes1.fr (E.K.); Tel.: +33-223-235-950 (J.-F.C.); +33-223-236-118 (E.K.)

Received: 3 November 2017; Accepted: 25 November 2017; Published: 27 November 2017

Abstract: The copolymerization of bio-renewable β-myrcene or β-farnesene with styrene was examined using an *ansa*-neodymocene catalyst, affording two series of copolymers with high styrene content and unprecedented syndioregularity of the polystyrene sequences. The incorporation of terpene in the copolymers ranged from 5.6 to 30.8 mol % (β-myrcene) and from 2.5 to 9.8 mol % (β-farnesene), respectively. NMR spectroscopy and DSC analyses suggested that the microstructure of the copolymers consists of 1,4- and 3,4-poly(terpene) units randomly distributed along syndiotactic polystyrene chains. The thermal properties of the copolymers are strongly dependent on the terpene content, which is easily controlled by the initial feed. The terpolymerization of styrene with β-myrcene in the presence of ethylene was also examined.

Keywords: copolymerization; rare-earth catalyst; styrene; β-myrcene; farnesene; ethylene; bio-sourced monomers; stereocontrol; syndiotactic

1. Introduction

The sustainability and possible eco-compatibility of bio-based polymers has raised much interest in finding inexpensive alternatives to petroleum-sourced materials. Among the wide variety of renewable monomers, terpenes are particularly interesting because of their abundance in nature, and their reactive conjugated 1,3-diene framework. For instance, β-myrcene, or to a lesser extent β-farnesene, can polymerize via anionic or radical polymerization to form elastomeric materials [1]. In a few rare cases, the coordination (catalytic) polymerization of such monomers has been reported [2–6]. On the other hand, syndiotactic polystyrene (sPS) is a very attractive material due to its high melting point (ca. 270 °C), high crystallinity, low dielectric constant and good chemical and heat resistances [7,8]. However, its processability is limited by its high melting point and its brittleness. Syndioselective copolymerization of styrene with small amounts of a second monomer is one of the most common ways to tune the properties of sPS, and thus to improve its processability [9–11]. A few examples of styrene-myrcene polymers have already been reported, mostly via anionic or radical copolymerizations [12–14]. To our knowledge, only one paper has addressed the coordination copolymerization of styrene with β-myrcene (My) in the presence of the ternary system

$Cp^*La(BH_4)_2(THF)_2$/*n*BuEtMg/Al*i*Bu$_3$, affording poly(S-*co*-1,4-*trans*-My) containing high amounts of myrcene (66–96 mol %) [15]. Yet, nothing has been reported about styrene-myrcene copolymers containing stereoregular PS sequences, nor about the copolymerization of styrene with *β*-farnesene.

Very recently, we reported new neutral allyl {Cp/Flu}-type neodymium and samarium complexes of the type {$R_2C(C_5H_4)$(R'R'Flu)}Ln(1,3-$C_3H_3(SiMe_3)_2$)$(THF)_x$ (Flu = 9-fluorenyl) that act as single-component catalysts for homo- and copolymerization of styrene with ethylene, featuring high syndioselectivity, good productivities and good control over the incorporated ethylene content [16]. Previous work conducted by our group also demonstrated syndioselective styrene/isoprene (/ethylene) co(ter)polymerizations using the neutral {(Me_2C(Cp)(Flu)}Nd(C_3H_5)(THF) complex [17]. In this paper, we report on the copolymerization of styrene with *β*-myrcene or farnesene with such catalyst systems. The synthesis of new poly(S-*co*-My) and poly(S-*co*-Fa) copolymers with high styrene content and containing syndiotactic polystyrene sequences is described. Styrene/ethylene/*β*-myrcene terpolymerizations were also attempted.

2. Results and Discussion

2.1. Homopolymerization of Myrcene and Farnesene

Homopolymerization of *β*-myrcene with {$Me_2C(C_5H_4)$(2,7-*t*Bu_2Flu)}Nd(1,3-$C_3H_3(SiMe_3)_2$)(THF) (**1**) in the presence of 10 equiv of (*n*Bu)$_2$Mg as scavenger was first assessed (Table 1, entries 1 and 2) [16]; this showed, however, very low productivity (0.74 kg·mol^{-1}·h^{-1} at 60 °C; 5.0 kg·mol^{-1}·h^{-1} at 120 °C). Signals in the ^{1}H NMR spectrum of the recovered poly(My) recorded in 1,1,2,2-tetrachloroethane-d_2 were assigned using the previously reported NMR data for poly(*β*-myrcene) samples [4,18]. Two distinct signals at δ 4.82 and 5.19 ppm revealed the presence of both 1,4- and 3,4-sequences (Figure 1). A 50:50 ratio of 1,4-/3,4- was obtained at T_{polym} = 60 °C; an increase of the polymerization temperature induced an increase in 3,4-insertions (1,4-/3,4- = 25:75 for T_{polym} = 120 °C, see the Supporting Information, Figure S1). The $^{13}C\{^1H\}$ NMR spectrum also showed characteristic signals corresponding to both 1,4- and 3,4-regioinsertions (Supporting Information, Figures S2 and S3); however, the resolution was not sufficient to distinguish unambiguously the signals corresponding to *cis*- and *trans*-1,4 insertions. The molecular weight of the poly(My) was determined by GPC (gel permeation chromatography) and found to be relatively low (M_n = 3900 g·mol^{-1}). DSC (differential scanning calorimetry) analyses revealed a T_g of ca. −58 °C, consistent with a 50:50 ratio of 1,4- and 3,4-segments [4,15]. Farnesene homopolymerization was also explored (Table 1, entries 11 and 12); however, the productivities were even lower than for *β*-myrcene homopolymerization (0.28–0.34 kg·mol^{-1}·h^{-1}) and a lower monomer loading was required to recover some poly(Fa) (i.e., $[Fa]_0/[Nd]_0$ = 200 instead of $[My]_0/[Nd]_0$ = 1000). NMR data recorded for the recovered polymer were consistent with those reported in the literature [6,19], and revealed a poly(Fa) microstructure made of a mixture of 1,4- and 3,4-insertions (Supporting Information, Figures S6 and S7). Note that some of those poly(Fa) materials were found to be hardly or even not at all soluble in most of the common solvents (CH_2Cl_2, $CHCl_3$, THF, 1,2,4-trichlorobenzene), possibly due to the presence of reticulated materials. Thus, DSC and GPC analyses were most often uninformative.

Table 1. Styrene/β-myrcene and styrene/farnesene copolymerizations catalyzed by **1** [a].

Entry	Comonomer	$[St]_0$ [M]	$[St]_0/[Nd]$	$[Comon]_0/[St]_0$	T_{polym} [°C]	Time [min]	Prod. [b] [kg·mol^{-1}·h^{-1}]	Conv. St [%]	Conv. Comon [%]	Comon. Inc. [c] [mol %]	T_m [d] [°C]	T_c [d] [°C]	T_g [d] [°C]	ΔH_m [d] [J·g^{-1}]	$M_n \times 10^{-3}$ [g·mol^{-1}] [e]	$Đ_M$ [e]
1 [f]	My	-	0	∞	60	1320	0.74	-	11.6	100	*no*	*no*	−58	*no*	3.87	1.33
2 [f]	My	-	0	∞	120	1320	5.0	-	78.8	100	*no*	*no*	−44	*no*	5.43	1.53
3	-	4.4	8000	0	60	120	248	60	-	0	251,265	231	100	30.0	22.6 [k]	2.5 [k]
4	My	4.4	8000	0.125	60	120	127	28.2	13.1	5.6	208,226	176	73	14.4	23.2	1.8
5 [g]	My	4.4	16,000	0.125	60	120	114	12.6	6.2	5.7	220,235	187	78	20.4	26.8	1.4
6	My	4.4	8000	0.25	60	120	56	11.6	5.7	10.9	206	156	70	9.9	25.1	1.3
7 [h]	My	4.4	20,000	0.25	120	120	374	27.1	26.7	19.7 [g]	no	no	45	no	30.3	1.8
8	My	4.4	8000	0.5	60	180	20	5.4	2.4	18.1	*no*	*no*	48	*no*	36.6	2.7
9 [i]	My	4.4	4000	0.5	60	180	54	29.2	14.8	20.0	*no*	*no*	33	*no*	28.2	2.3
10	My	3.3	6000	1	60	360	6.4	3.9	1.7	30.8	*no*	*no*	12	*no*	35.3	2.3
11 [j]	Fa	-	0	∞	60	1320	0.28	-	15.1	100	*nd*	*nd*	*nd*	*nd*	*nd*	*nd*
12 [j]	Fa	-	0	∞	120	1320	0.34	-	18.6	100	*nd*	v	*nd*	*nd*	*nd*	*nd*
13	Fa	4.4	8000	0.125	60	120	198	45.1	9.4	2.5	246 257	214	83	29.2	31.4 [k]	3.9 [k]
14	Fa	4.4	8000	0.125	120	240	234	>99	30.0	3.4	227	165	86	23.1	18.4 [k]	2.2 [k]
15	Fa	4.4	8000	0.25	60	120	84	19.2	1.6	2.0	243 257	224	85	31.1	20.8 [k]	3.6 [k,*]
16	Fa	3.8	7000	0.5	60	180	31	11.5	1.1	4.7	225 241	204	66	18.4	14.7 [k]	2.3 [k]
17	Fa	2.7	5000	1	60	360	28	26.6	2.9	9.8	212	149	63	9.0	14.4 [k]	2.9 [k]

[a] General conditions unless otherwise stated: 10 µmol of **1**; solvent = cyclohexane (T_{polym} = 60 °C) or *n*-dodecane (T_{polym} = 120 °C); [Nd] = 5.4×10^{-4} mol·L^{-1}; $[Mg(nBu)_2]/[Nd]$ = 10; styrene, β-myrcene and farnesene (75:25 mixture of α- and β-isomers) purified through neutral alumina, stirring on CaH_2, trap-to-trap vacuum distillation and stored at −27 °C on 3 Å molecular sieves; *no*: not observed; [b] Productivity calculated over the whole reaction time; [c] Determined by ^{1}H NMR spectroscopy; [d] Determined by DSC from second run; [e] Determined by GPC at 30 °C in THF; [f] β-Myrcene homopolymerization, $[My]_0/[Nd]_0$ = 1000, [Nd] = 3.6×10^{-3} mol·L^{-1}, $[My]_0$ = 3.6 mol·L^{-1}; [g] [Nd] = 2.7×10^{-4} mol·L^{-1}; [h] [Nd] = 2.2×10^{-4} mol·L^{-1}; [i] [Nd] = 1.1×10^{-3} mol·L^{-1}; [j] Farnesene homopolymerization, $[Fa]_0/[Nd]_0$ = 200, [Nd] = 1.6×10^{-2} mol·L^{-1}, $[Fa]_0$ = 3.2 mol·L^{-1}; [k] Determined by GPC at 135 °C in 1,2,4-trichlorobenzene; * Bimodal distribution.

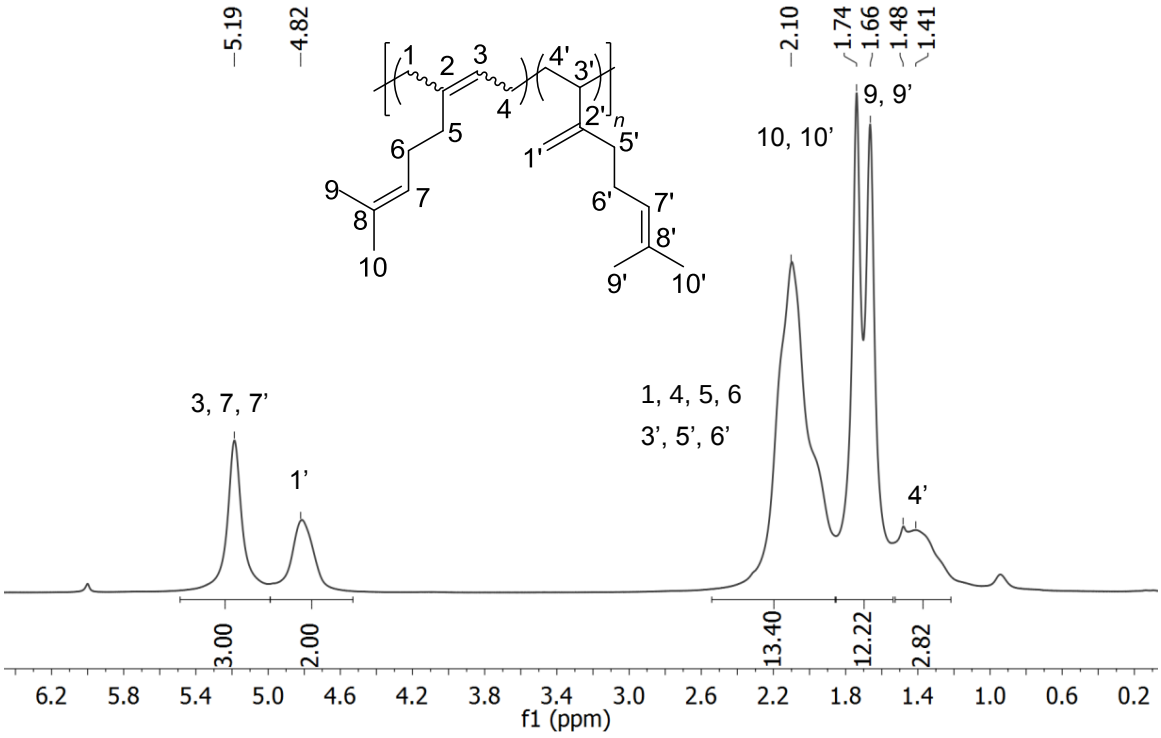

Figure 1. ^{1}H NMR spectrum (500 MHz, 1,1,2,2-tetrachloroethane-d_2, 60 °C) of a poly(β-myrcene) prepared with **1** (Table 1, entry 1).

2.2. Copolymerizations of Styrene with β-Myrcene and Farnesene

A series of styrene/β-myrcene and styrene/farnesene copolymerizations catalyzed by **1** were performed (Scheme 1, Table 1).

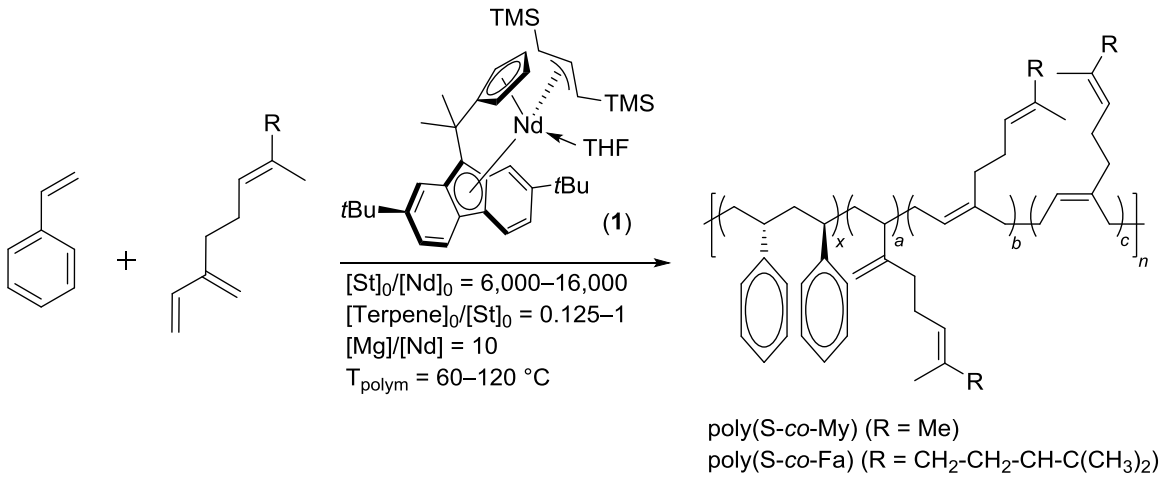

Scheme 1. Styrene/β-myrcene and styrene/farnesene copolymerizations catalyzed by complex **1** (Table 1, entries 4–10 and entries 13–17).

As judged by the relatively narrow monomodal molecular weight distributions ($Đ_M$ = 1.3–2.7), true copolymers were produced. Depending on the quantity of incorporated β-myrcene, the resulting copolymers were either white powders or transparent hard elastomeric materials. On the other hand, all poly(S-*co*-Fa) samples were white powders. The catalyst productivity decreased with an increase of the [terpene]$_0$/[St]$_0$ feed ratio (from 127 to 6.4 kg·mol^{-1}·h^{-1} and from 198 to 28 kg·mol^{-1}·h^{-1} in the

cases of styrene/β-myrcene and styrene/farnesene copolymerization, respectively, entries 4–10 and entries 13–17); this is consistent with the fact that **1** is poorly active towards β-myrcene and farnesene homopolymerization (entries 1–2 and 11–12). On the other hand, as the $[terpene]_0/[St]_0$ feed ratio was raised, the terpene content in the resulting copolymers increased as expected; thus, a wide range of compositions was obtained (My content = 5.6–30.8 mol % and Fa content = 1.5–9.8 mol %). It should be noted that, under similar copolymerization conditions, the incorporation of farnesene in the copolymer is 2–3 times lower than the incorporation of β-myrcene (for instance, compare entries 4 and 13 or 10 and 17). This difference is due to the fact that commercially available farnesene is a mixture of α- and β-isomers (ca. 75:25 mixture of α/β; see Figure S21); however, only the β-isomer was incorporated, as evidenced from the ^{1}H NMR data (see the Supporting Information, Figure S12), whereas the initial ratio $[Fa]_0/[St]_0$ was calculated considering the entire amount of farnesene (i.e., both α- and β-isomers). We assume that the trisubstituted C^3=C bond in the α-isomer, as compared to the disubstituted C^3=C one in the β-isomer, most likely accounts for lower reactivity of the α-isomer (selective polymerization of β-farnesene was already reported in the literature; see [6]). In addition, an increase in polymerization temperature logically induced an increase in productivity (6 times higher when going from 60 °C to 120 °C in the case of styrene/β-myrcene copolymerization), but also an increase in the amount of terpene incorporated in the copolymer (from 10.9 to 19.7 mol % and from 2.0 to 3.4 mol % for β-myrcene and β-farnesene, respectively; entries 6 and 7 and entries 13–14, respectively).

The reactivity ratios of r_{ST} = 2.06 and r_{MY} = 0.37 were determined according to the Fineman−Ross equation (Supporting Information, Figure S8) [20]. These values indicate a preference for the insertion of styrene, regardless of the last inserted monomer unit, consistent with the fact that **1** is 3 orders of magnitude more productive in catalyzing styrene homopolymerization than in catalyzing β-myrcene homopolymerization (entries 1 and 3) [21].

Microstructures of the copolymers were examined by $^{13}C\{^1H\}$ NMR spectroscopy (Figure 2). Single and relatively sharp signals in the *ipso* carbon (δ 145.2 ppm) and methylene (δ 43.8 ppm) regions of the spectra are indicative of the presence of poly(S-*co*-My) and poly(S-*co*-Fa) with sPS sequences. These signals broadened with an increase of terpene content, due to the increasing presence of styrene-terpene junctions (see Figure 3 for poly(S-*co*-My) copolymers and Supporting Information, Figure S14, for poly(S-*co*-Fa) copolymers). Note that the spectra were recorded using a regular NMR sequence that does not necessarily return quantitative signals; thus, the syndiotacticity content was not quantified. In addition, the presence of both 1,4- and 3,4-units for both copolymers confirms that complex **1** is not regioselective towards β-myrcene or β-farnesene. The non-regioselectivity of **1** in those St/My and St/Fa copolymerizations contrasts with styrene/isoprene copolymers containing regular *trans*-1,4-polyisoprene units obtained in the presence of $\{CpCMe_2Flu\}Nd(C_3H_5)(THF)$ [17]. We assume that this arises from the more sterically hindered C^3=C bond in the higher β-myrcene and β-farnesene monomers and/or from the presence of 2,7-*tert*-butyl substituents on the fluorenyl moiety of catalyst **1**. The presence of a unique T_g for all co- and terpolymers suggests a random distribution of comonomers within sPS segments (consistent with the aforementioned broadening of ^{13}C NMR signals due to increasing presence of styrene-terpene junctions).

As expected, properties of the copolymers were dependent on their composition, which is easily tunable by adjusting the monomer feed ratio. The T_g values significantly decreased with the increase of β-myrcene and β-farnesene contents (Figure 4), and poly(S-*co*-My) materials incorporating between 10 and 20 mol % of β-myrcene units were completely amorphous. As compared with isoprene-based copolymers [17], a wider range of thermal properties is potentially available using these terpenes as comonomers. As shown in Figure 4, the T_g values of the three copolymers were similar at low comonomer incorporation levels (T_g = 70–77 °C for 3–9 mol % of comonomer inserted). For higher amounts of comonomer incorporated (15–30 mol %), the T_g values of poly(S-*co*-My) copolymers monotonously decreased, while those of poly(S-*co*-1,4-*trans*-IP) reached a plateau at ca. 60 °C.

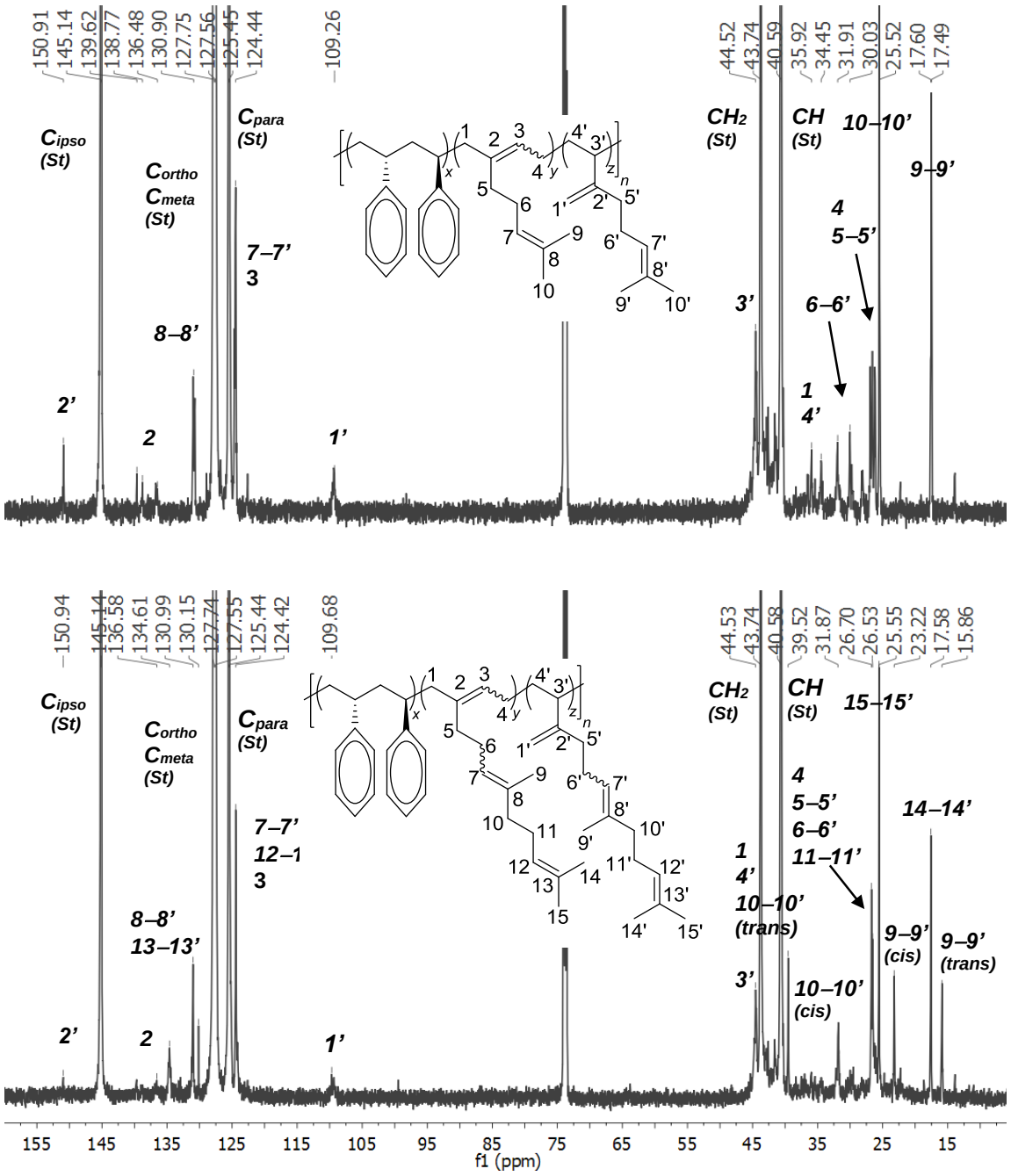

Figure 2. $^{13}C\{^{1}H\}$ NMR spectra (125 MHz, 1,1,2,2-tetrachloroethane-d_2, 60 °C) of a poly(S-*co*-My) copolymer (top) (Table 1, entry 6), and a poly(S-*co*-Fa) copolymer (bottom) (Table 1, entry 16), with proposed signal assignment.

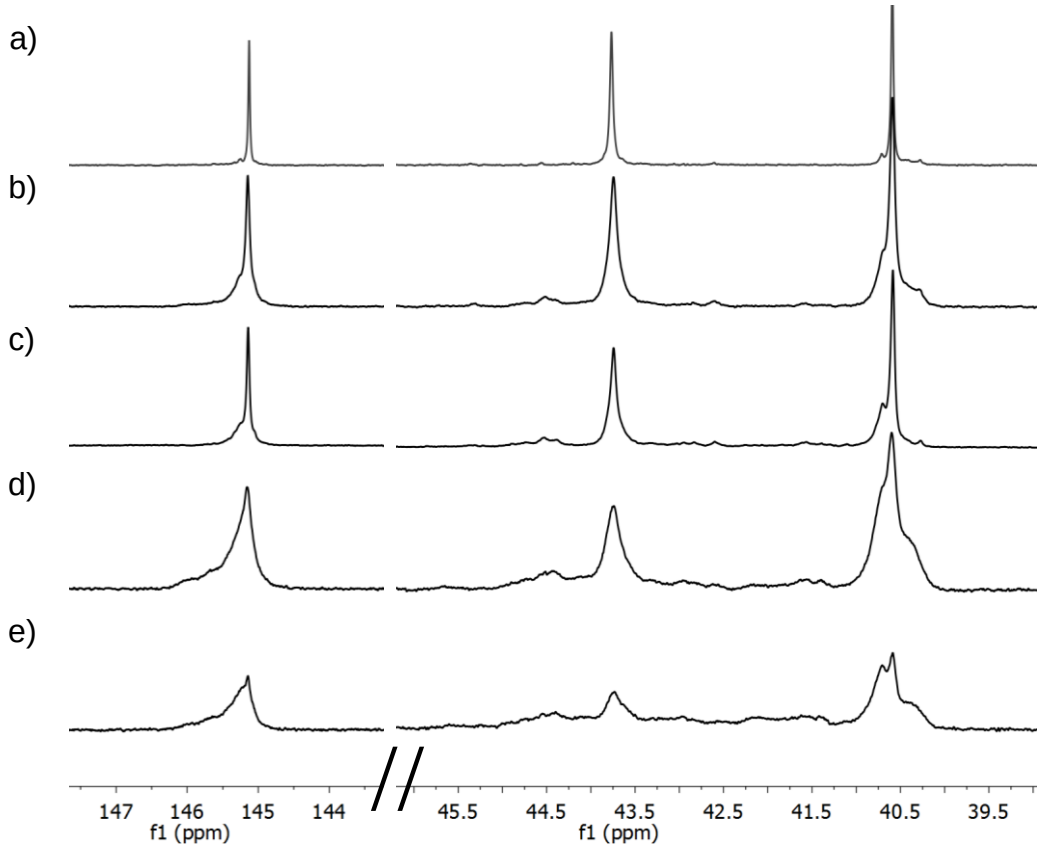

Figure 3. Stack-plot of detailed regions (left, *ipso*; right: methylene carbon) of the $^{13}C\{^{1}H\}$ NMR spectra (125 MHz, 1,1,2,2-tetrachloroethane-d_2, 60 °C) of poly(S-*co*-My) copolymers (Table 1): (**a**) pure sPS (Table 1, entry 3); (**b**) 5.6 mol % of *β*-myrcene (entry 4); (**c**) 10.9 mol % of *β*-myrcene (entry 6); (**d**) 18.1 mol % of *β*-myrcene (entry 8); (**e**) 30.8 mol % of *β*-myrcene (entry 10).

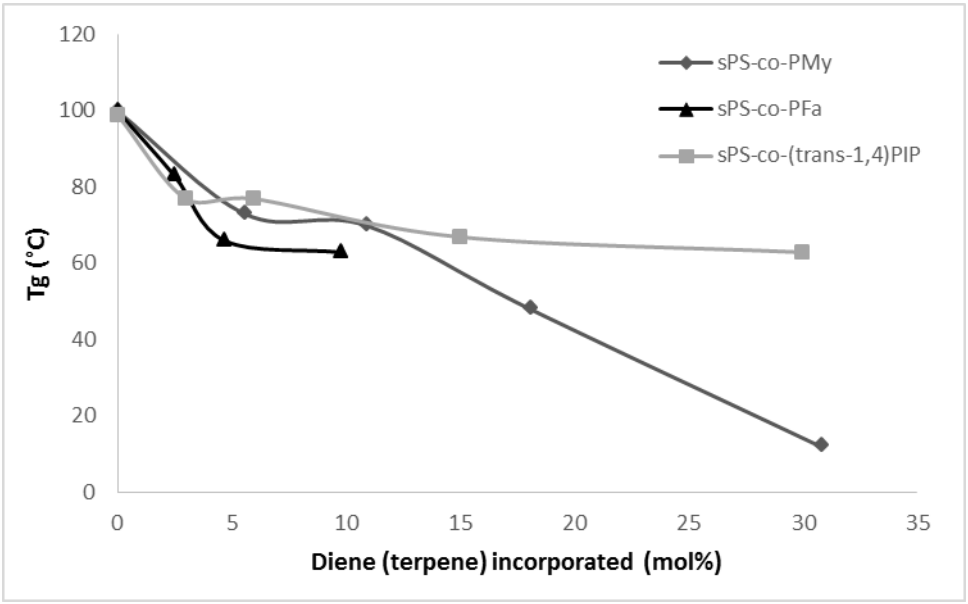

Figure 4. Variation of the glass transition temperature (T_g) of poly(S-*co*-My), poly(S-*co*-Fa) and poly(S-*co*-1,4-*trans*-IP) [17] copolymers as a function of diene (terpene) comonomer content (Table 1, entries 3, 4, 6, 8, 10, 13, 15, 16).

2.3. Terpolymerizations of Styrene with β-Myrcene and Ethylene

A series of styrene/β-myrcene/ethylene terpolymerizations was also performed under the same conditions (Scheme 2, Table 2). The remarkably narrow and monomodal molecular weight distributions suggested the formation of true terpolymers ($Đ_M$ = 1.3–1.6). Complex **1** was moderately productive for styrene/β-myrcene/ethylene terpolymerizations (64–250 kg·mol^{-1}·h^{-1}), and the productivity decreased with an increase in the $[My]_0/[St]_0$ feed ratio. However, it is noteworthy that these productivities were significantly higher than those obtained for styrene/β-myrcene copolymerizations under the same conditions (6–127 kg·mol^{-1}·h^{-1}, compare Tables 1 and 2). This difference in productivity between co- and terpolymerizations is even more pronounced with the increase of $[My]_0/[St]_0$, as productivity values were 2–10 fold larger in terpolymerization than in the corresponding copolymerization. This can be accounted for by the fact that ethylene is a smaller, less sterically demanding monomer than styrene or β-myrcene and, thus, is more easily inserted. Hence, ethylene acts as a "spacer" that facilitates subsequent insertions of styrene or β-myrcene monomer, resulting in higher overall productivities than in copolymerizations without ethylene [22–24]. Under the given conditions, the level of β-myrcene incorporated in terpolymers was equivalent to that observed for styrene/β-myrcene copolymers. In addition, the amount of ethylene incorporated in terpolymers increased (from 18.8 up to 29.2 mol %) with an increase in β-myrcene content.

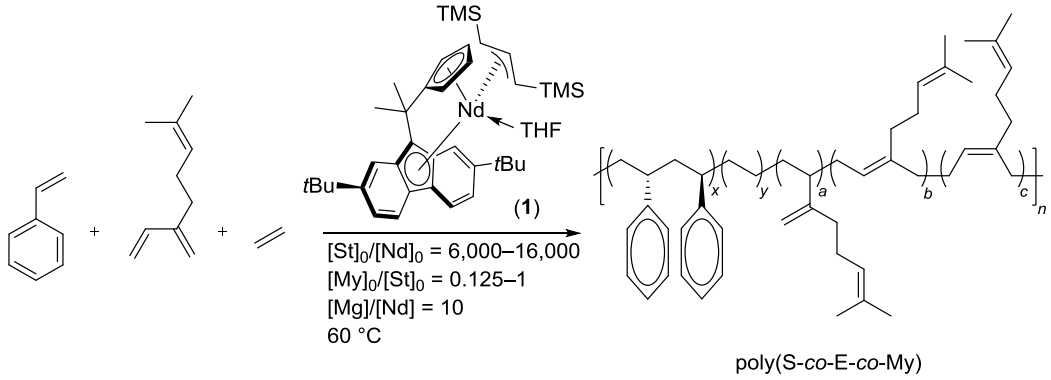

Scheme 2. Styrene/β-myrcene/ethylene terpolymerizations catalyzed by **1.**

Table 2. Styrene/β-myrcene/ethylene terpolymerizations catalyzed by **1** [a].

Entry	$[St]_0$ [M]	$[St]_0/[Ln]$	$[My]_0/[St]_0$	Time [min]	Prod. [b] [kg·mol^{-1}·h^{-1}]	C2 Inc. [c] [mol %]	My Inc. [c] [mol %]	T_m [d] [°C]	T_c [d] [°C]	T_g [d] [°C]	ΔH_m [d] [J·g^{-1}]	$M_n \times 10^{-3}$ [g·mol^{-1}] [e]	$Đ_M$ [e]
1	4.4	8000	0.125	120	250	18.8	4.9	*no*	*no*	61	*no*	38.2	1.31
2 [f]	4.4	16,000	0.125	120	255	19.4	4.3	*no*	*no*	63	*no*	45.3	1.6
3	4.4	8000	0.25	120	167	22.4	9.1	*no*	*no*	58	*no*	35.9	1.29
4	4.4	8000	0.5	180	123	24.2	20.2	*no*	*no*	2	*no*	122.1	1.5
5	3.3	6000	1	360	64	29.2	31.1	*no*	*no*	−21	*no*	87.6	1.5
6 [h]	4.4	8000	-	120	>400	9.5	-	218	151	87	15.0	44.6 [g]	1.9 [g]

[a] General conditions unless otherwise stated: 27–54 μmol of **1**; [Nd] = 5.4 × 10^{-4} mol·L^{-1}; $[Mg(nBu)_2]/[Nd]$ = 10; T_{polym} = 60 °C; $P_{ethylene}$ = 2 bar; styrene and β-myrcene purified through neutral alumina, stirring on CaH_2, trap-to-trap vacuum distillation and stored at −27 °C on 3 Å molecular sieves; *no*: not observed; [b] Productivity calculated over the whole reaction time; [c] Determined by ^{1}H NMR spectroscopy; [d] Determined by DSC from second run; [e] Determined by GPC at 30 °C in THF; [f] [Nd] = 2.7 × 10^{-4} mol·L^{-1}; [g] Determined by GPC at 135 °C in 1,2,4-trichlorobenzene; [h] Styrene-ethylene copolymerization performed under similar conditions.

The poly(S-*co*-E-*co*-My) terpolymers were also characterized by $^{13}C\{^1H\}$ NMR spectroscopy (Supporting Information, Figure S18). As previously observed for styrene/β-myrcene copolymers, PS sequences in the terpolymers were predominantly syndiotactic (see the *ipso* carbon signal at δ 145.2 ppm) and the myrcene units were present as both 1,4- and 3,4-units (for instance, see the resonances at δ 150.9 and 138.6–136.7 ppm assigned to the C2 atom of the backbone of 3,4- and 1,4-insertions, respectively). Again, the T_g values were significantly lower in poly(S-*co*-E-*co*-My)

terpolymers than in poly(S-*co*-E-*co*-1,4-*trans*-IP) terpolymers (at a given ethylene incorporation level, ca. 20 mol %) [17]. The T_g values were also lower in poly(S-*co*-E-*co*-My) terpolymers than in poly(S-*co*-My) copolymers containing similar β-myrcene incorporation contents.

3. Materials and Methods

General considerations. All experiments were performed under a dry argon atmosphere, using a glovebox or standard Schlenk techniques. Cyclohexane and *n*-dodecane were distilled from CaH_2 and stored over 3 Å molecular sieves. Toluene was distilled from Na/K alloy and stored over 3 Å molecular sieves. 1,1,2,2-Tetrachloroethane-d_2 (TCE-d_2, 99% D, Acros Organics, Geel, Belgium) was used as received. Styrene (Fisher Chemical, Waltham, MA, USA general purpose grade, stabilized with 10–15 ppm of *tert*-butylcatechol) was eluted through neutral aluminum oxide, stirred and heated over CaH_2, vacuum-distilled and stored over 3 Å molecular sieves at −30 °C under argon. β-Myrcene (Acros Organics, Geel, Belgium, technical grade, stabilized with 0.01% of α-Tocopherol) and farnesene (75:25 α/β mixture of isomers, generously provided by Total Raffinage-Chimie) was dried over CaH_2, transferred by trap-to-trap under vacuum and stored at −30 °C under argon. (nBu)$_2$Mg (1.0 M solution in hexanes, Sigma-Aldrich, Lyon, France) was used as received. Ethylene (Air Liquide, Paris, France, N35) was used without further purification.

Instruments and measurements. ^{1}H and ^{13}C{^{1}H} NMR spectra of co- and terpolymers were recorded on a Bruker AM-500 spectrometer (1,1,2,2-tetrachloroethane-d_2, 60 °C, Bruker, Wissembourg, France). GPC analyses of β-myrcene-based polymers were performed in THF at 30 °C using PS standards for calibration. GPC analyses of farnesene-based polymers were performed in 1,2,4-trichlorobenzene at 135 °C using PS standards for calibration. Differential scanning calorimetry analyses were performed on a Setaram DSC 131 apparatus (SETARAM Instrumentation, Cranbury, NJ, USA), under continuous flow of helium and using aluminum capsules. Crystallization temperatures were measured during the first cooling (10 °C.min^{-1}), and glass transition and melting temperatures were measured during the second heating (10 °C.min^{-1}).

Typical procedure for styrene-terpene copolymerization. In a typical experiment (Table 1, entry 4), complex **1** (ca. 8 mg), cyclohexane (7.6 mL) and (nBu)$_2$Mg (0.1 mL of a 1.0 M solution in hexanes) were introduced in the glovebox in a Schlenk flask. The tube was capped with a septum. Out of the glovebox, the tube was heated with an oil bath at 60 °C. Under vigorous stirring, styrene (9.4 mL) and β-myrcene (1.8 mL) were added with syringes. When the desired polymerization time was reached, methanol (10 mL) was added to quench the reaction. The precipitated polymer was washed with methanol (ca. 50 mL), filtered and dried under vacuum at 60 °C until constant weight was reached.

Typical procedure for styrene/β-myrcene/ethylene terpolymerization. In a typical experiment (Table 2, entry 1), a 300 mL-glass high-pressure reactor (TOP-Industrie, Vaux le Pénil, France) was charged with cyclohexane (41 mL) under argon and heated at the appropriate temperature by circulating water in a double mantle. Under an ethylene flow were introduced styrene (50 mL), β-myrcene (9.4 mL), and (nBu)$_2$Mg (0.5 mL of a 1.0 M solution in hexanes) and the solution of complex **1** in toluene (ca. 43 mg in 2 mL). The ethylene pressure in the reactor was kept constant at 2 bar with a back regulator and the reaction media was mechanically stirred. At the end of the polymerization, the reactor was vented to air, and the copolymer was precipitated in methanol (ca. 500 mL), washed with methanol and dried under vacuum at 60 °C until constant weight was reached.

Calculation of β-myrcene and styrene fractions in poly(S-*co*-My) copolymers. The fraction of β-myrcene and styrene F_{My} and F_{St} in the copolymers was calculated with the following equations:

$$F_{St} = A_{arom}/5 \quad (1)$$

$$F_{My} = (A_{aliph} - 3(A_{arom}/5))/13.5 \quad (2)$$

where A_{aliph} is the area of aliphatic hydrogens (δ 0.5–2.5 ppm) and A_{arom} is the area of aromatic hydrogens of styrene (δ 6.5–7.5 ppm). The fraction of β-myrcene can also be determined by considering the area of olefinic hydrogens A_{olefin} (δ 4.0–5.5 ppm) but the uncertainty in the integration of the latter signals is more important than using the aliphatic hydrogens signals.

Calculation of β-farnesene and styrene fractions in poly(S-*co*-Fa) copolymers. The fraction of β-farnesene and styrene F_{Fa} and F_{St} in copolymers was calculated with the following equations:

$$F_{St} = A_{arom}/5 \quad (3)$$

$$F_{Fa} = (A_{aliph} - 3(A_{arom}/5))/20.5 \quad (4)$$

where A_{aliph} is the area of aliphatic hydrogens (δ 0.5–2.5 ppm) and A_{arom} is the area of aromatic hydrogens of styrene (δ 6.5–7.5 ppm).

Calculation of β-myrcene and styrene fractions in poly(S-*co*-E-*co*-My) terpolymers. Styrene, β-myrcene and ethylene fractions in terpolymers were calculated using the following equations:

$$F_{St} = A_{arom}/5 \quad (5)$$

$$F_{My} = A_{olefin}/2.5 \quad (6)$$

$$F_{Eth} = (A_{aliph} - 3(A_{arom}/5) - 13.5(A_{olefin}/2.5))/4 \quad (7)$$

where A_{aliph} is the area of aliphatic hydrogens (δ 0.5–2.5 ppm) and A_{arom} is the area of aromatic hydrogens of styrene (δ 6.5–7.5 ppm).

4. Conclusions

In this contribution, we reported on the production of new poly(S-*co*-My) copolymers and poly(S-*co*-E-*co*-My) terpolymers using a highly productive and syndioselective *ansa*-lanthanidocene catalyst previously described by our group. The incorporation level and the overall catalytic productivity were somewhat lower as compared to analogous styrene/isoprene copolymerizations. The composition of the final polymers was easily controlled by adjusting the initial feed ratio; thus, a wide range of materials with various thermal properties was obtained. In particular, terpene-based co- and terpolymers featured a wider range of T_g values compared with isoprene-based co(ter)polymers already reported by our group (at a given diene incorporation level) [17], indicating the potentially easier processability of those new materials.

Supplementary Materials: Supporting Information is available online at http://www.mdpi.com/2073-4344/7/12/361/s1. Figure S1: ^{1}H NMR spectrum (400 MHz, 25 °C, TCE-d_2) of poly(My) (T_{polym} = 120 °C, Table 1, entry 2), Figure S2: $^{13}C\{^1H\}$ NMR spectrum (125 MHz, 60 °C, TCE-d_2) of poly(My) (T_{polym} = 60 °C, Table 1, entry 1), Figure S3: $^{13}C\{^1H\}$ NMR spectrum (100 MHz, 25 °C, TCE-d_2) of poly(My) (T_{polym} = 120 °C, Table 1, entry 2), Figure S4: DSC thermogram of poly(My) (Table 1, entry 1), Figure S5: GPC trace of poly(Fa) (Table 1, entry 1), Figure S6: ^{1}H NMR spectrum (500 MHz, 60 °C, TCE-d_2) of poly(Fa) (Table 1, entry 11), Figure S7: $^{13}C\{^1H\}$ NMR spectrum (125 MHz, 60 °C, TCE-d_2) of poly(Fa) (Table 1, entry 11), Figure S8: Fineman-Ross plot for the copolymerizations of styrene and myrcene with **1**/(nBu)$_2$Mg at 60 °C and least-square best-fit line (F = [St]/[My] in feed, f = [St]/[My] in copolymer), Figure S9: Typical ^{1}H NMR spectrum (500 MHz, 60 °C, TCE-d_2) of poly(S-*co*-My) (Table 1, entry 8), Figure S10: DSC thermogram of poly(S-*co*-My) (Table 1, entry 8), Figure S11: GPC trace of poly(S-*co*-My) (Table 1, Entry 8), Figure S12: ^{1}H NMR spectra (400 MHz, 25 °C, $CDCl_3$) of farnesene: before styrene-farnesene copolymerization (top), after styrene-farnesene copolymerization (bottom) (Table 1, entry 4), Figure S13: Typical ^{1}H NMR spectrum (500 MHz, 60 °C, TCE-d_2) of poly(S-*co*-Fa) (Table 1, entry 17), Figure S14: Stack-plot of detailed regions (left, ipso; right: methylene carbon) of the $^{13}C\{^1H\}$ NMR spectra (125 MHz, TCE-d_2, 60 °C) of poly(S-*co*-Fa) copolymers (Table 1): (a) pure sPS (Table 1, entry 3); (b) 2.5 mol % of farnesene (entry 13); (c) 3.4 mol % of farnesene (entry 14); (d) 4.7 mol % of farnesene (entry 16); (e) 9.8 mol % of farnesene (entry 17); Figure S15: DSC thermogram of poly(S-*co*-Fa) (Table 1, entry 14); Figure S16: GPC trace of poly(S-*co*-Fa) (Table 1, entry 14); Figure S17: Typical ^{1}H NMR spectrum (500 MHz, 60 °C, TCE-d_2) of poly(S-*co*-E-*co*-My) (Table 2, entry 3), Figure S18: Typical $^{13}C\{^1H\}$ NMR spectrum (125 MHz, 60 °C, TCE-d_2) of poly(S-*co*-E-*co*-My) (Table 2, entry 3); Figure S19: DSC thermogram of poly(S-*co*-E-*co*-My) (Table 2, entry 3);

Figure S20. GPC trace of poly(S-*co*-E-*co*-My) (Table 2, entry 3); Figure S21: ^{1}H NMR spectrum (400 MHz, $CDCl_3$, 25 °C) of farnesene as a mixture of α- and β-isomers.

Acknowledgments: This work was gratefully supported by Total SA and Total Research and Technology Feluy (Ph.D. grant to E. Laur).

Author Contributions: Jean-François Carpentier and Evgueni Kirillov designed the study and the experiments. Eva Laur performed the experiments and analyses. Eva Laur, Jean-François Carpentier and Evgueni Kirillov interpreted the experiments and wrote the manuscript. Alexandre Welle, Aurélien Vantomme and Jean-Michel Brusson helped in co-supervision of the study.

Conflicts of Interest: The authors declare no conflict of interest.

References and Notes

1. Behr, A.; Johnen, L. Myrcene as a natural base chemical in sustainable chemistry: A critical review. *ChemSusChem* **2009**, *2*, 1072–1095. [PubMed]
2. Loughmari, S.; Hafid, A.; Bouazza, A.; El Bouadili, A.; Zinck, P.; Visseaux, M. Highly stereoselective coordination polymerization of β-myrcene from a lanthanide-based catalyst: Access to bio-sourced elastomers. *J. Polym. Sci. Part A Polym. Chem.* **2012**, *50*, 2898–2905.
3. Díaz de León Gómez, R.E.; Enríquez-Medrano, F.J.; Maldonado Textle, H.; Mendoza Carrizales, R.; Reyes Acosta, K.; López González, H.R.; Olivares Romero, J.L.; Lugo Uribe, L.E. Synthesis and characterization of high *cis*-polymyrcene using neodymium-based catalysts. *Can. J. Chem. Eng.* **2016**, *94*, 823–832.
4. Liu, B.; Li, L.; Sun, G.; Liu, D.; Li, S.; Cui, D. Isoselective 3,4-(co)polymerization of bio-renewable myrcene using NSN-ligated rare-earth metal precursor: An approach to a new elastomer. *Chem. Commun.* **2015**, *51*, 1039–1041. [CrossRef] [PubMed]
5. Liu, B.; Han, B.; Zhang, C.; Li, S.; Sun, G.; Cui, D. Renewable β-myrcene polymerization initiated by lutetium alkyl complexes ligated by imidophosphonamido ligand. *Chin. J. Polym. Sci.* **2015**, *33*, 792–796.
6. Raynaud, J.; Wu, J.Y.; Ritter, T. Iron-catalyzed polymerization of isoprene and other 1,3-dienes. *Angew. Chem. Int. Ed.* **2012**, *51*, 11805–11808. [CrossRef] [PubMed]
7. Schellenberg, J. *Syndiotactic Polystyrene: Synthesis, Characterization, Processing, and Applications*; John Wiley & Sons: Hoboken, NJ, USA, 2010.
8. Malanga, M. Syndiotactic polystyrene materials. *Adv. Mater.* **2000**, *12*, 1869–1872.
9. Zinck, P.; Bonnet, F.; Mortreux, A.; Visseaux, M. Functionalization of syndiotactic polystyrene. *Prog. Polym. Sci.* **2009**, *34*, 369–392.
10. Jaymand, M. Recent progress in the chemical modification of syndiotactic polystyrene. *Polym. Chem.* **2014**, *5*, 2663–2690.
11. Laur, E.; Kirillov, E.; Carpentier, J.-F. Engineering of syndiotactic and isotactic polystyrene-based copolymers *via* stereoselective catalytic polymerization. *Molecules* **2017**, *22*, 594.
12. Quirk, R.P.; Huang, T.-L. Alkyllithium-initiated polymerization of myrcene: New block copolymers of styrene and myrcene. In *New Monomers and Polymers*; Polymer Science and Technology; Culbertson, B.M., Pittman, C.U., Jr., Eds.; Springer: Boston, MA, USA, 1984; Volume 25, pp. 329–355.
13. Sarkar, P.; Bhowmick, A.K. Terpene based sustainable elastomer for low rolling resistance and improved wet grip application: Synthesis, characterization and properties of poly(styrene-*co*-myrcene). *ACS Sustain. Chem. Eng.* **2016**, *4*, 5462–5474. [CrossRef]
14. Métafiot, A.; Kanawati, Y.; Gérard, J.-F.; Defoort, B.; Marić, M. Synthesis of β-myrcene-based polymers and styrene block and statistical copolymers by SG1 nitroxide-mediated controlled radical polymerization. *Macromolecules* **2017**, *50*, 3101–3120. [CrossRef]
15. Georges, S.; Touré, A.O.; Visseaux, M.; Zinck, P. Coordinative chain transfer copolymerization and terpolymerization of conjugated dienes. *Macromolecules* **2014**, *47*, 4538–4547. [CrossRef]
16. Laur, E.; Louyriac, E.; Dorcet, V.; Welle, A.; Vantomme, A.; Miserque, O.; Brusson, J.-M.; Maron, L.; Carpentier, J.-F.; Kirillov, E. Substitution effects in highly syndioselective styrene polymerization catalysts based on single-component allyl *ansa*-lanthanidocenes: An experimental and theoretical study. *Macromolecules* **2017**, *50*, 6539–6551.

17. Rodrigues, A.-S.; Kirillov, E.; Vuillemin, B.; Razavi, A.; Carpentier, J.-F. Stereocontrolled Styrene–isoprene copolymerization and styrene–ethylene–isoprene terpolymerization with a single-component allyl *ansa*-neodymocene catalyst. *Polymer* **2008**, *49*, 2039–2045. [CrossRef]
18. Georges, S.; Bria, M.; Zinck, P.; Visseaux, M. Polymyrcene microstructure revisited from precise high-field nuclear magnetic resonance analysis. *Polymer* **2014**, *55*, 3869–3878. [CrossRef]
19. Newmark, R.A.; Majumdar, R.N. ^{13}C-NMR spectra of *cis*-polymyrcene and *cis*-polyfarnesene. *J. Polym. Sci. Part A Polym. Chem.* **1988**, *26*, 71–77.
20. Fineman, M.; Ross, S.D. Linear method for determining monomer reactivity ratios in copolymerization. *J. Polym. Sci.* **1950**, *5*, 259–262. [CrossRef]
21. Due to the fact that the ratio of α/β isomers of farnesene in the monomer was not exactly known and that only the β-isomer was polymerized, the reactivity ratios related to the styrene-farnesene copolymerization could not be determined.
22. Tan, R.; Guo, F.; Li, Y. Copolymerization of propylene with styrene and ethylene by a THF-containing half-sandwich scandium catalyst: Efficient synthesis of polyolefins with a controllable styrene content. *Polym. Chem.* **2017**, *4*, 482–489. [CrossRef]
23. Li, X.; Hou, Z. Scandium-catalyzed copolymerization of ethylene with dicyclopentadiene and terpolymerization of ethylene, dicyclopentadiene, and styrene. *Macromolecules* **2005**, *38*, 6767–6769.
24. Guo, F.; Nishiura, M.; Koshino, H.; Hou, Z. Cycloterpolymerization of 1,6-heptadiene with ethylene and styrene catalyzed by a THF-free half-sandwich scandium complex. *Macromolecules* **2011**, *44*, 2400–2403. [CrossRef]